Mechanism of Formin-Induced Nucleation of Actin Filaments

Martin Pring,[‡] Marie Evangelista,[§] Charles Boone,[§,||] Changsong Yang,[⊥] and Sally H. Zigmond*[,⊥]

Department of Physiology, University of Pennsylvania, Philadelphia, Pennsylvania, 19104-6085, Department of Biology, Queen's University, Kingston, Ontario, K7L 3N6 Canada, Banting and Best Department of Medical Research and Department of Molecular and Medical Genetics, University of Toronto, Toronto, Ontario M5G 1L6 Canada, and Biology Department, University of Pennsylvania, Philadelphia, Pennsylvania 19104-6018

Received July 25, 2002; Revised Manuscript Received November 15, 2002

ABSTRACT: A fragment of the yeast formin Bni1 containing the FH1FH2 domains increases the rate of filament nucleation from pure G-actin [Pruyne et al. (2002) *Science 297*, 612−615]. To determine the mechanism of nucleation, we compared the G-actin dependence of Bni1FH1FH2-induced polymerization with theoretical models. The data best fit a model suggesting that Bni1FH1FH2 stabilizes an actin dimer. We also show that nucleation increases with the square root of the Bni1FH1FH2 concentration. We demonstrate that this relationship is expected for any such nucleator, independent of nucleus size. The proline-rich FH1 domain binds profilin, and deletion of this domain decreases the contribution of profilin−actin to the nucleation. A role for profilin binding to the FH1 domain in filament nucleation was supported by the inability of Bni1FH1FH2 to utilize a mutant profilin, H133S profilin, with defective binding to polyproline. Bni1FH1FH2 partially inhibits barbed-end elongation, and we find that the rate constants for both polymerization and depolymerization are decreased by approximately 50%. Bni1FH1FH2 has no effect on pointed-end kinetics or on the critical concentration. To investigate the domains of Bni1 required for these activities, the experiments were all duplicated with the FH2 domain alone. The FH2 domain is as effective as the FH1FH2 domains together in inhibiting barbed-end kinetics; it is less effective as a nucleator but the mechanism is again best fit by dimer stabilization.

In vivo, most polymerization occurs at the barbed end of an actin filament. The location of polymerization is thus determined by the location of free barbed-end elongation sites (*1*). A free barbed end can be created by severing or uncapping an existing filament or by de novo nucleation. Because spontaneous nucleation is very slow at the concentrations of free G-actin[1] present in cytoplasm, additional factors such as the Arp2/3 complex or formins are required to facilitate de novo nucleation (*1*−*3*). To understand how this facilitation occurs, it is helpful to first consider spontaneous nucleation

Spontaneous nucleation of G-actin occurs under physiological conditions but exhibits a substantial lag time even at [G-actin] levels well above those believed to exist in cells. It is generally accepted that the G-actin dimer and trimer are unstable, with dissociation constants ∼0.1 M for actin dimers and 10^{-5} to 10^{-4} M for actin trimers (*1*). Tobacman and Korn (*4*) have proposed a nucleation/polymerization model that, though probably somewhat simpler than reality, fits such data well with a small number of adjustable parameters that have a clear mechanistic interpretation. The model defines a filament as an oligomer with n or more monomers that both elongates and depolymerizes with rate constants characteristic of F-actin. It assumes that the largest unstable oligomer, with $n - 1$ monomers, is in equilibrium with free G-actin and elongates with an F-actin rate constant (see Results for equations). This largest unstable oligomer (an $(n - 1)$-mer) is described as the nucleus.[2] For spontaneous nucleation of MgATP−G-actin under physiological conditions these authors found that a model with $n = 4$, i.e., a trimer as the nucleus, best fit their data.

A number of F-actin-binding proteins that bind a filament better than a monomer, e.g., coronin (*5*), members of the Ena/VASP family (*6*, *7*), and the S-1 fragment of myosin (*8*), increase the rate of nucleation in vitro. In many cases the nucleation by these factors remains slow or is detected only under unphysiological conditions such as low salt (e.g., the S-1 fragment of myosin, VASP) or high G-actin concentrations. Thus, it is not clear if these factors actually nucleate filaments in vivo or rather function by stabilizing and/or cross-linking filaments.

Many factors that bind/cap the end of a filament can also nucleate a new filament. Thus, barbed-end capping factors, including gelsolin, cytochalasin (*9*), and capping protein (*10*), also bind G-actin monomers and/or unstable oligomers and increase the rate of nucleation. By stabilizing oligomers, they increase the concentration of nuclei that are available to

[†] S.H.Z. and C.Y. are supported by NIH Grant AI19883. M.E. and C.B. are supported by NCIC grants.

* Corresponding author. E-mail: szigmond@sas.upenn.edu. Tel.: 215-898-4559. Fax: 215-898-8780.

[‡] Department of Physiology, University of Pennsylvania. E-mail: pringm@dolphin.upenn.edu.

[§] Queen's University.

[||] University of Toronto.

[⊥] Biology Department, University of Pennsylvania.

[1] Abbreviations: VCA, verprolin, cofilin, acidic domains of N−Wiscott Adrich Syndrom protein; G-actin, monomeric actin; FH1, formin homology 1 domain; FH2, formin homology 2 domain.

[2] This nomenclature, now in common use, deviates from that introduced by Tobacman and Korn, who applied the term nucleus to the smallest stable oligomer, or *n*-mer.

10.1021/bi026520j CCC: $25.00
Published on Web 12/17/2002

elongate and reduce the value of *n* below that for spontaneous nucleation. However, since these filaments are capped at their barbed ends, they must elongate at their pointed ends, making it unlikely that these factors contribute to nucleation in vivo. On the other hand the Arp2/3 complex, which can cap the pointed end, nucleates filaments able to elongate at their barbed ends (*11*). Its function has been demonstrated to be important in vivo (*12*).

Formins are also important for nucleation in vivo. In mammals, formins function downstream of Rho to form focal contacts and stress fibers (*13*−*15*). In yeast they function downstream of Cdc42 and other Rho proteins to induce actin cables in an Arp2/3-independent manner (*16*−*20*). In addition, they are used at cytokinesis to form the acto-myosin based contractile ring (*21*−*23*). Their function appears to include nucleation of new actin filaments. The C-terminal of the yeast formin Bni1 containing the FH1 and FH2 domains is sufficient to nucleate actin filaments in vitro (*2*, *3*). The FH2 domain is critical for nucleation in vitro (*2*).

Interestingly, the FH1FH2 domains of Bni1 also cap the barbed end, decreasing but not blocking the rate of polymerization (*2*). The formin cap at the barbed end may help to anchor filaments at the bud tip where the cables converge. Bni1 localizes to the bud tip (*17*). The filaments of the cable are presumed to be oriented with their barbed ends at the tip since myosin V mediates movement of vesicles along the cable to the bud tip (*24*). The bud tip also appears to be the site of cable polymerization since a bleached spot in cable bound GFP-Abp140 moves toward the mother cell (*25*).

In vivo, formation of cables depends on profilin which binds to proline-rich ligands (*16*). All formins contain a proline-rich FH1 domain that occurs adjacent and NH2-terminal to the FH2 domain, and for several formins has been shown to bind profilin (*22*). Profilin is not needed for nucleation by FH1FH2 in vitro (*2*, *3*). Why profilin is required in vivo is not yet clear.

In this manuscript we investigate the mechanism of nucleation by FH1FH2 and the contribution of profilin.

MATERIALS AND METHODS

Bni1 Constructs. Bni1FH1FH2 (AA 1227−1824) and Bni1FH2 (AA 1348−1824) were expressed as GST-fusion proteins as described (*2*). Since cleavage of the GST from FH1FH2 had no effect on its nucleating activity (*2*), it was used as a GST-fusion protein. On the other hand, the activity of GST-FH2 was increased by thrombin cleavage of the GST (*2*), so it was cleaved before use. Throughout this paper FH1FH2 refers to GST-Bni1FH1FH2 and FH2 refers to Bni1FH2.

Actin. Rabbit skeletal muscle actin was prepared from rabbit muscle acetone powder as described by Young et al. (*26*). The actin was filtered on a sepharose column, and fractions with high nucleating activity were removed before the actin was pooled and frozen in aliquots in liquid nitrogen, stored at −80 °C, and defrosted as described (*26*). The actin was used within 7 days of thawing. Pyrenyl labeling of muscle actin was carried out according to Kouyama and Mihashi (*27*) with the modifications described by Northrop et al. (*28*). Pyrenylactin stored at 4 °C was stable for several months. Preliminary experiments demonstrated that nucleation by FH1FH2 was more efficient with MgATP−actin than with CaATP−actin; thus, for experiments analyzing the early time course of nucleation, actin, stored as CaATP−actin was pre-converted to MgATP−actin by incubation for 5 min in enough EGTA to be in excess of the calcium plus 50 μM $MgCl_2$. FH1FH2-induced nucleation was also slightly better with unlabeled than pyrene-labeled actin; thus, the pyrenylactin was added only to the level needed to obtain satisfactory results, 0% for nucleation experiments (where pyrenylactin was needed only after dilution) and between 4% and 50% (as needed for resolution) in the polymerization experiments (see below).

Gelsolin was isolated from serum according to the method of Cooper (*29*). Gelsolin−actin seeds were prepared by incubating gelsolin and actin (1/100 ratio) in polymerization buffer including 0.1 mM $CaCl_2$ to activate the gelsolin. The number of filaments produced was determined from the gelsolin concentration and from the rate of polymerization they induced using a pointed-end on rate of 1/μM/s. Both methods gave similar results. Spectrin−actin seeds, used as a stable source of free barbed ends, were isolated according to Casella et al. (*30*) and stored in 50% glycerol at −20 °C. The concentration of free barbed ends was estimated from the rate of polymerization induced using a barbed end on rate of 10/μM/s.

Nucleation assays were performed as published, with the exception that we used Mg−G-actin (*2*, *31*). The number of filaments produced during a given incubation was determined by diluting 50-fold into 0.5 μM pyrenylactin and measuring the initial rate of increase of pyrenylactin fluorescence (ex_{370}, em_{410}). Because 0.5 μM actin is similar to the critical concentration of the pointed end, there is no elongation from pointed ends. The number concentration of filaments was calculated using the measured change in fluorescence per μM F−actin, an on rate of 10/μM/s, and a critical concentration of 0.1 μM.

Polymerization assays were performed by following polymerization of actin spiked with pyrenylactin as described (*2*).

*Profilins. W*ild-type profilin1 (human), H133S profilin, and R74E profilin were expressed in *Escherichia coli* as GST-constructs as described (*32*). The effective concentrations of the wild type and H133S preparations were determined by assaying inhibition of elongation from gelsolin-seeds (see below), using a K_d of profilin for actin of 0.1 μM as shown previously (*32*). Because profilin−actin cannot add to the pointed end of a filament, the rate of elongation from gelsolin−actin seeds is proportional to the free G-actin concentration. Approximately 83% of the wild type profilin preparation and 66% of the H133S-profilin preparation were able to bind actin. This assay cannot be used for R74E-profilin, which does not bind actin; thus, its concentration was based solely on the protein concentration.

Supernatant of Yeast Lysates. Yeast (*S. cerevisiae*) strains (wt, YEF473; *arp2*Δ, RLY574, and its control, RLY1) were grown at room temperature on YPD medium. After they reached a density of 1.5−2 at OD_{600}, they were resuspended at 5×10^8 cells/mL in intracellular physiological (IP) buffer (135 mM KCl, 10 mM NaCl, 2 mM MgCl2, 2 mM EGTA, 10 mM Hepes, pH 7.1) with protease inhibitors (1 μg/mL leupeptin, 1 μg/mL benzamidine, 10 μg/mL aprotinin). Cells were lysed by passing cells through a French pressure cell at 2000 psi. The high-speed supernatant (HSS) was made

by spinning at 80 000 rpm for 20 min (~5.6 × 10^6 g/min) in a Beckman TL 100 centrifuge using a 100 rotor. The supernatant was removed and frozen in 150 μL aliquots with liquid nitrogen.

RESULTS

Nucleation by FH1FH2 Occurs via Dimer Stabilization. GST-Bni1FH1FH2 (FH1FH2) accelerates actin nucleation such that at high concentration there is no detectable lag (*2*). To investigate the mechanism of formin-enhanced nucleation, we examined the G-actin dependence of polymerization induced by FH1FH2. Since preliminary experiments demonstrated that FH1FH2 induced nucleation sites much more readily from Mg−G-actin than from Ca−G-actin, the actin was converted to Mg−actin immediately before use. The time course of polymerization induced by 75 nM FH1FH2 was determined at several initial G−actin concentrations (Figure 1A). The data were then fit to a model of FH1FH2-stimulated polymerization (*4*) in which the nucleus contained one, two, or three actin monomers[3]

$$\frac{d[N]}{dt} = k_n[FH1FH2][G]^{n-1}([G] - c_\infty)$$

$$\frac{d[G]}{dt} = -k_+[N]([G] - c_\infty) - n\frac{d[N]}{dt}$$

where [G] = [G-actin]; [N] = filament number concentration; $n - 1$ = nucleus size.

The value of k_+ was set to 5 × 10^6 M^{-1} s^{-1} (1 × 10^7 M^{-1} s^{-1}, 50% inhibited by FH1FH2, see below). Experiments to determine the extent of sequestration of G-actin by FH1FH2 showed that it was below the threshold for quantitation (G-actin pelleting with GST-FH1FH2 beads suggest a K_d > 5 μM; data not shown, and Figure 5 below), so the concentration of FH1FH2 was taken as that initially added. The data were best fit by a model where the FH1FH2 stabilized a dimer, making a trimer the smallest oligomer with the same on and off rates as a filament (Figure 1A,B). Data from polymerization induced by the smaller fragment, FH2, also were best fit by a model with $n = 3$, although the preference of $n = 3$ over $n = 4$ in this case was smaller (not shown). The composite constant k_n does not distinguish between dimer stabilization by capture of a dimer or sequential binding of two G-actin monomers.[4]

Nucleation by FH1FH2 was thus similar to that observed for cytochalasin, which is also characterized by $n = 3$ and considered to stabilize a dimer (*9*) and to that observed for capping protein (*10, 33*). It contrasts with that of VCA-activated Arp2/3 where addition of a single actin via the verprolin domain is thought to be sufficient to form a stable F-actin-like nucleus (Figure 1B).

Nucleation is a Function of [FH1FH2]$^{0.5}$. In hope of shedding further light on the mechanism, we next examined the dependence of nucleation on the concentration of FH1FH2. The maximum rate did not increase linearly with FH1FH2 concentration but rather increased less steeply at

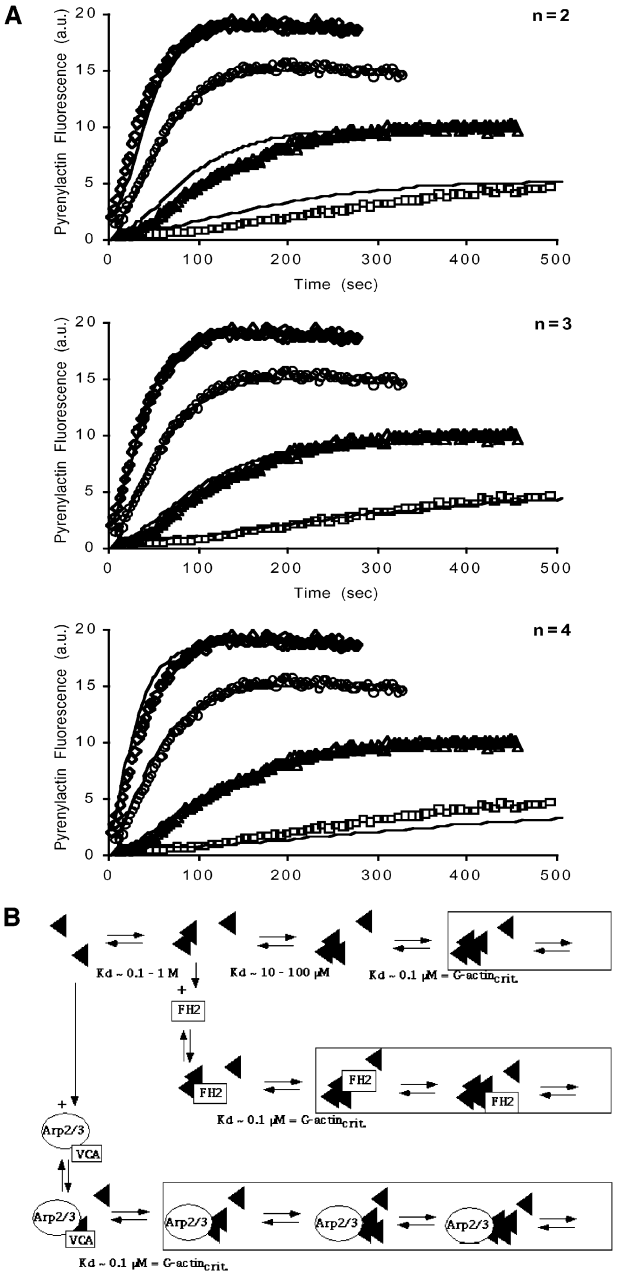

FIGURE 1: (A) Nucleation occurs by actin dimer stabilization. FH1FH2-induced polymerization as a function of [G-actin] was fit by polymerization models with different nucleus sizes. Magnesium−actin (containing 20% pyrenylactin) was induced to polymerize by addition of polymerization salts and 75 nM FH1FH2. Polymerization was followed from the pyrenylactin fluorescence (see Methods). The experimental data are shown as open symbols ([G-actin]: 1 μm, □; 2 μm, △; 3 μm, ○; 4 μm, ◇); the fit of the model for $n = 2$, 3, or 4 (see text) is shown with solid lines. Using a least-squares fit, the sum of squares of deviations for $n = 2$ was 278, for $n = 3$ it was 55, and for $n = 4$ it was 230 (arbitrary units). The k_n for $n = 3$ was estimated to be 7.05 × 10^{-5} $\mu M^3/s$. (B) Diagram of nucleation mechanisms. The figure illustrates how the stable oligomer size relates to spontaneous nucleation (top row), FH1FH2 or FH2-mediated nucleation (middle row) and Arp2/3-mediated nucleation (bottom row). In spontaneous nucleation, actin monomers (triangles) assemble into a very unstable dimer, a trimer (the nucleus), and finally a tetramer, which, along with all larger oligomers (boxed), has the same critical concentration as the filament. FH2, by stabilizing a dimer as the nucleus, decreases the nucleus size to two (note: the diagram is not meant to imply that FH2 has to bind a dimer rather than two monomers sequentially). Arp2/3 is activated by VCA, which also delivers a G-actin to form the nucleus, decreasing the nucleus size to one.

[3] The data were not corrected for spontaneous nucleation, which in each case was much slower than the induced rate, so that any correction would be negligible.

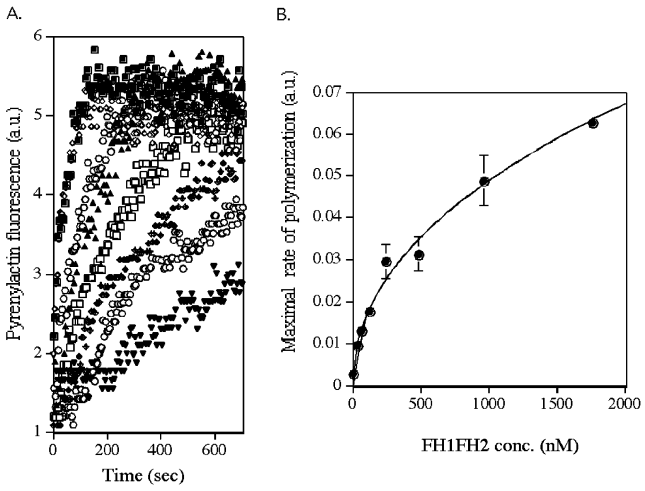

FIGURE 2: Polymerization as a function of [FH1FH2]. (A) Actin (2μM MgATP actin, 20% pyrenylactin) was induced to polymerize by addition of various concentrations of FH1FH2, from right to left: 0, 30, 60, 120, 240, 480, 960, 1760 nM, and the increase in pyrenylactin fluorescence was followed. (B) The maximal rate of polymerization for each curve was determined at the steepest point and plotted vs the FH1FH2 concentration present. The best fit to the data ($y = 0.002 \times 0.460$, $r^2 = 0.99$) indicated that the maximal rate was a function of the square root of [FH1FH2].

higher concentrations (Figure 2). Since G-actin was present in great excess and actin dimers are being created continuously, neither was being saturated by FH1FH2. Filament annealing could contribute to a decrease in ends at high concentration but would contribute little here since the decrease occurred when the concentration of filaments was less than nanomolar. The data were reasonably fit by a curve where the concentration of filaments at maximal polymerization was proportional to $[\text{FH1FH2}]^{\sim 0.5}$ (Figure 2 B). Published data were also fit by this relationship (*2*).

Examination of the equations that describe nucleation indicated that the concentration of filaments at peak polymerization is expected to be proportional to the square root of the nucleator concentration, and this is a general property of any nucleator that depends on the free G-actin concentration. Because the nucleated filaments elongate and thereby consume G-actin, the more filaments nucleated, the less time available for nucleation before the G-actin is depleted (see derivations in Appendix) (*34*). Thus, this feature of nucleation is not unique to FH1FH2 but rather a general property of nucleators and therefore provides no mechanistic information. Indeed, Arp2/3-induced nucleation as a function of Arp2/3 complex concentration also shows this relationship (Figure 6B in Higgs et al. (*35*)). At high levels of nucleation, annealing of the filaments produced also decreases the number present (*36*, *37*). We conclude that there is no saturation or inhibition of nucleation by concentrations of FH1FH2 $\leq$ 2 μM.

FH1FH2 Can Stimulate Filament Production in Supernatant of Lysed Yeast. Since dimer stabilization is a relatively inefficient means of nucleation when the G-actin concentration is low, we examined whether FH1FH2 could nucleate filaments in supernatant of lysed yeast with no added G-actin. Since cytoplasm is diluted in supernatant over that in the cell, the free G-actin concentration may be even lower than in vivo. Yet FH1FH2 did increase filament number in a dose-dependent manner (Figure 3A). FH2 was about as effective as FH1FH2 (Figure 3B). The number of filaments produced during a 5 min incubation with 0.2 μM FH1FH2 was about 20% of that induced by incubation with 0.1 μM VCA to activate the endogenous Arp2/3 complex (not shown). To determine if the nucleation by FH1FH2 in yeast supernatant depended on the presence of the Arp2/3 complex, we produced supernatant from cells lacking the arp2 subunit of the complex. VCA induced polymerization in wild-type supernatant (supplemented with 0.5 μM pyrenylactin to follow polymerization) but not from the *arp2*-null supernatant (Figure 3C and D). In contrast, FH1FH2-induced polymerization was similar in the presence or absence of arp2. Thus, consistent with in vivo data (*16*), FH1FH2 functions in cell supernatant in an Arp2/3 complex-independent manner.

Profilin−Actin Contributes to Nucleation if the FH1 Domain Is Present. Profilin binds to the FH1 domain and appears necessary for nucleation by formins in vivo (*17*). While profilin is not required for FH1FH2-induced nucleation in vitro (*2*, *3*), the requirement in vivo may reflect the fact that the profilin−actin concentration is higher than the free G-actin concentration (*1*, *32*). To determine if profilin−actin can promote nucleation by FH1FH2, we compared the nucleation ability of a solution of profilin−actin to that either with the same total G-actin concentration or with the same free G-actin concentration. We first determined the free G-actin concentration in the profilin−actin mixtures by examining elongation from the filament pointed ends using gelsolin seeds (see Methods, Figure 4B). Elongation from spectrin actin seeds confirmed that the presence of profilin did not inhibit barbed-end elongation (Figure 4A).

Defining the effect of profilin−actin on nucleation is complicated by the fact that profilin−actin contributes to barbed-end elongation and by the fact that profilin binds less well to pyrenylactin than to unlabeled actin. To bypass these complications, we incubated FH1FH2 with unlabeled actin or with a mixture of profilin and unlabeled actin (profilin−actin) for a set time and then determined the number of barbed ends present from the rate of polymerization follow-

[4] The composite constant k_n can be obtained in this case by the following derivation. We have these reactions:

$$\text{FH1FH2} + \text{G-actin} \overset{K_a}{\longleftrightarrow} \text{FH1FH2}-\text{G-actin}$$

$$\text{FH1FH2}-\text{G-actin} + \text{G-actin} \overset{K_b}{\longleftrightarrow} \text{FH1FH2}-(\text{G-actin})_2$$

$$2\text{G-actin} \overset{K_c}{\longleftrightarrow} (\text{G-actin})_2$$

$$\text{FH1FH2} + (\text{G-actin})_2 \overset{K_d}{\longleftrightarrow} \text{FH1FH2}-(\text{G-actin})_2$$

$$\text{FH1FH2}-(\text{G-actin})_2 + \text{G-actin} \overset{c_\infty}{\longleftrightarrow} \text{FH1FH2}-\text{F-actin}$$

where all of the constants are dissociation constants and

$$c_\infty = k_-/k_+$$

then k_n is given by

$$k_n = \frac{k_+}{K_a K_b} = \frac{k_+}{K_c K_d}$$

Any set of individual rate constants for the formation and breakdown of the nucleus (and any complexes that precede it) must obey the following conditions: (1) they are compatible with the observed k_n, (2) they are sufficiently rapid to predict that equilibrium would occur, and (3) they comply with physical constraints (e.g., diffusion limitation). In this case these individual constants cannot be defined without additional information or assumptions.

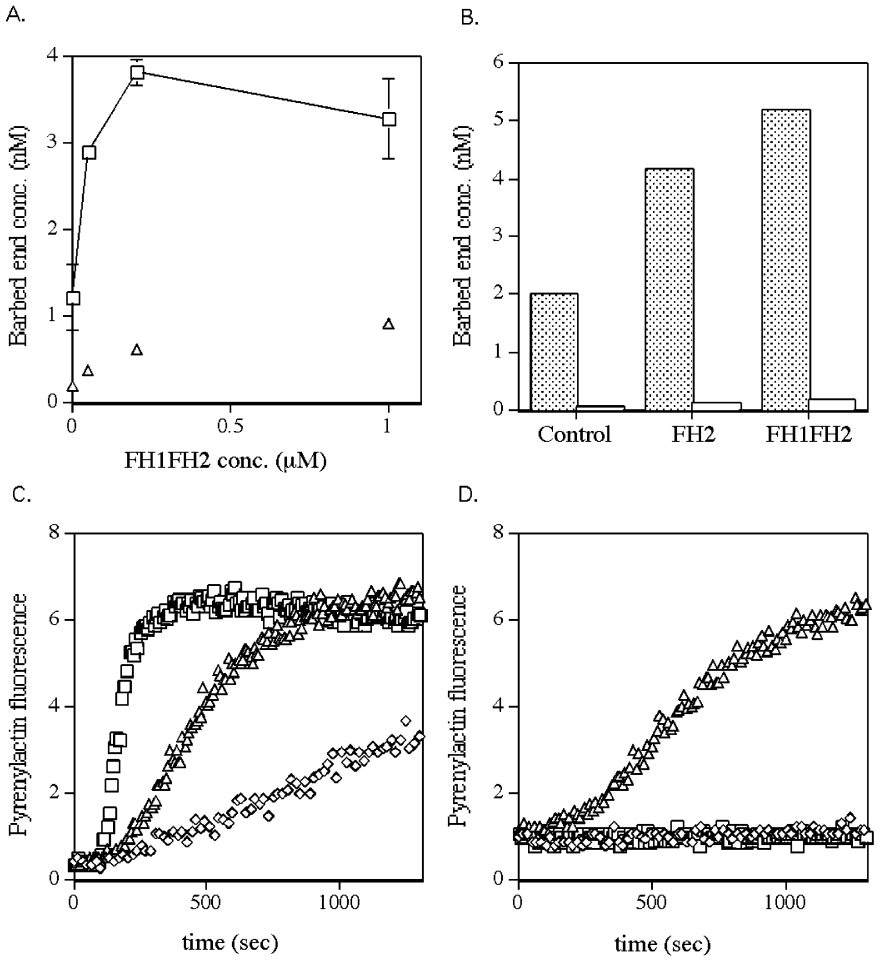

FIGURE 3: Nucleation by FH1FH2 in yeast supernatant. (A) Filament barbed ends were assayed after incubation of different concentrations of FH1FH2 with wild-type high-speed supernatant (at 6 mg/mL, no added actin) for 1 min (triangles) or 5 min (squares) before 20-fold dilution into 0.5 μM pyrenylactin (see Methods). The rate of elongation determined from the rate of increase in pyrenylactin fluorescence is proportional to the number of barbed ends. (B) Filament ends were assayed after incubation of wild-type supernatant (at 6 mg/mL, no added actin) for 5 min at room temperature with addition of buffer (control) or 200 nM FH2 or 200 nM FH1FH2. Barbed ends were measured from the rate of polymerization after 20-fold dilution into 0.5 μM pyrenylactin. Open bars are control samples incubated with no supernatant. (C and D) Polymerization was induced by VCA at 0.1 μM (squares), FH1FH2 at 0.2 μM (triangles), or no addition (diamonds) in high-speed supernatant (at 1 mg/mL) from wild type (C) or *arp2-null* cells (D) spiked with 0.5 μM pyrenylactin to allow polymerization to be monitored.

ing a 50-fold dilution of the sample into 0.5 μM pyrenylactin (Figure 4C,D). Controls incubated without FH1FH2 determined the extent of spontaneous nucleation. The contributions of actin, profilin and FH1FH2, added after dilution, were negligible (not shown).

FH1FH2 induced more filaments when incubated with profilin−actin than with the concentration of G-actin that remained free in the profilin−actin mixture but less than that with the same total G-actin in the mixture (Figure 4C). Thus, profilin−actin can contribute to nucleation but less efficiently than free G-actin. To determine if interaction between profilin and the polyproline region of FH1 contributed to the nucleation, we repeated the experiment using a mutant form of profilin, H133S-profilin, which supports barbed-end elongation similarly to wild type profilin (Figure 4A) but binds polyproline poorly (*32*, *38*). FH1FH2-induced nucleation with H133S−profilin−actin was no greater than that with the same free G-actin (Figure 4C), indicating that interaction between the FH1 domain and profilin was necessary for profilin to enhance nucleation.

To confirm this, we examined nucleation by FH2. Since FH2 is a less efficient nucleator than FH1FH2 (*2*), we first determined the concentration of FH2 that gave a rate of nucleation with pure G-actin comparable to that of 75 nM FH1FH2 (250 nM FH2 approximately matched (see actin samples in Figure 4C,D)). We then examined the ability of FH2 to nucleate in the presence of profilin or H133S profilin. The extent of nucleation observed with wild type and with H133S profilin were similar and not greater than that with the same free G-actin (Figure 4D).

To determine if profilin binding to the FH1 domain stabilized an active conformation or positioned a bound G-actin to contribute to nucleation, we examined whether nucleation by FH1FH2 could be enhanced by R74E-profilin, which binds to the polyproline domain but poorly to G-actin (*32*). The presence of R74E had little effect on FH1FH2-induced nucleation in either 1.6 or 4 μM G-actin (Figure 4E). Because R74E profilin binds G-actin weakly, it did not lower the free G-actin concentration, and nucleation was determined by the total G-actin. Therefore, binding of profilin

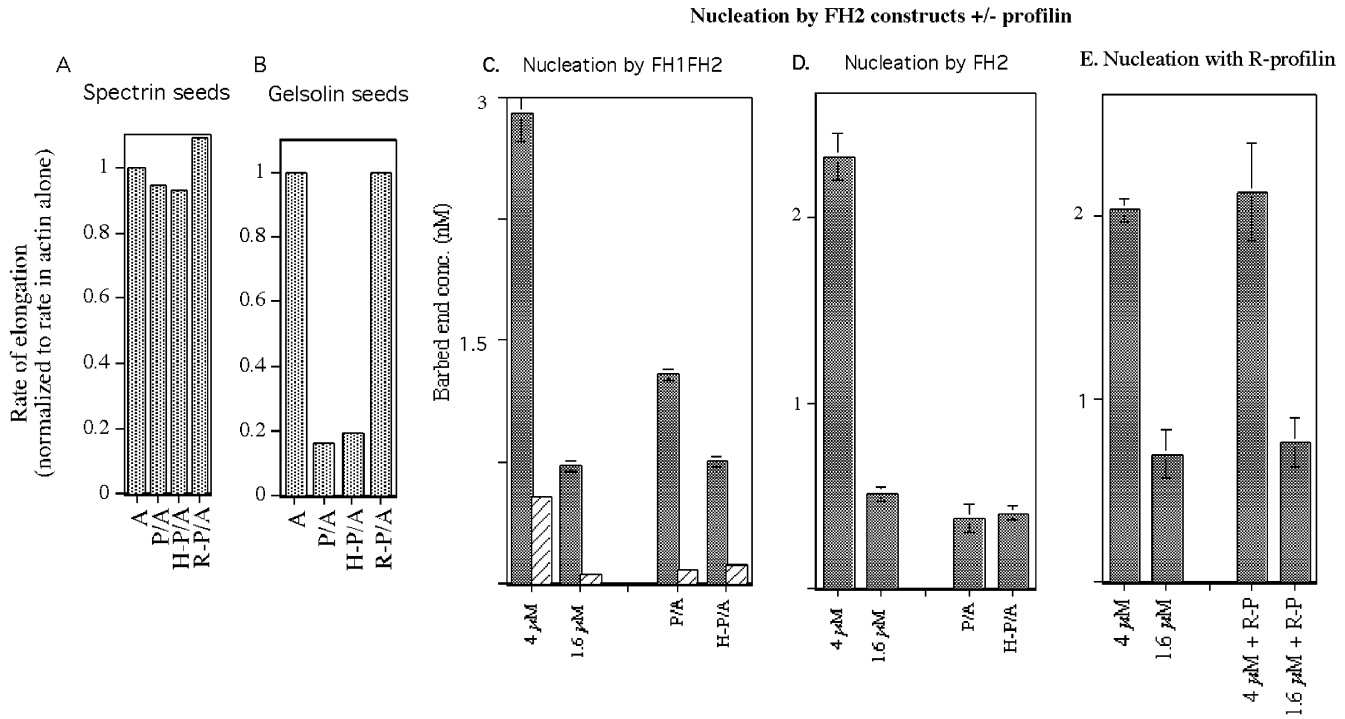

FIGURE 4: (A and B) Characterization of profilin effect on barbed-end and pointed-end elongation. (A) Profilin, H133S profilin, and R74E profilin do not significantly decrease the rate of elongation from spectrin seeds. The rate of elongation from ~1 nM seeds was determined in 4 μM actin (10% pyrenylactin) ± 2.5 μM wild-type profilin (P/A), H133S profilin (H-P/A), or R74E profilin (R-P/A). The samples were normalized to the rate in actin alone. (B) To determine experimentally the concentration of free G-actin in a mixture of profilin and actin, we examined the decrease in the rate of elongation from the pointed end using gelsolin capped filaments as nucleation sites with 4 μM actin alone (10% pyrenylactin) or in the presence of 2.5 μM wild type, H133S profilin, and R74E profilin (see Methods). The rate of elongation from the pointed end in the presence of profilin is determined by the difference between the free actin concentration and the critical concentration. By estimating the G-actin concentration from the relative rates and then examining the rate of elongation nucleated by gelsolin seeds in different concentrations of pure G-actin, the free G-actin present with wild type and H133S profilin was determined to be 1.6 μM. As expected from its inability to bind G-actin, R74E profilin did not decrease the rate of elongation relative to the 4 μM actin alone. (C−E) Nucleation by FH1FH2 and FH2 with profilin−actin. (C) To examine nucleation by FH1FH2 in the presence of profilin−actin, G-actin, 4 μM or 1.6 μM (0% labeled), was incubated without (light bars) or with FH1FH2 (75 nM) (dark bars) for 4 min and the number of ends determined (from the rate of elongation following 50× dilution into 0.5 μM pyrenylactin). The same concentration of FH1FH2 was then incubated with 4 μM G-actin plus profilin (2.5 μM) (P/A) or H133S profilin (2.5 μM) (H-P/A), concentrations that gave a free G-actin = 1.6 μM (see Figure 4B). Data plotted are means and range of duplicates. This experiment is representative of four independent experiments. (D) FH2 (250 nM) was incubated as in panel A with 4 or 1.6 μM G-actin or 4 μM G-actin with wild-type profilin (P/A) or H133S profilin (H-P/A) as described above. In this case, neither wild type nor H133S profilin increased nucleation over the free G-actin control. Data plotted are means and range of duplicates. This experiment is representative of three independent experiments. (E) FH1FH2 (75) nM was incubated with 4 or 1.6 μM G-actin without or with 2.5 μM R74E profilin (R-P/A) before dilution and assay of ends as in Figure 3C. Data shown are the means and duplicate range.

to the FH1 domain does not appear to activate FH1FH2. Rather, binding of profilin−actin via the polyproline region of the FH1 domain appears necessary for profilin−actin to participate in nucleation.

The FH2 Domain is Critical for Capping. FH1FH2 has the surprising ability to partially cap the barbed end of actin filaments (*2*). We found that this inhibition was limited to the barbed end since there was no inhibition of pointed-end elongation nucleated by gelsolin seeds (Figure 5A−C). Although the FH2 domain is a less effective nucleator than FH1FH2, it was equally effective at inhibiting barbed-end elongation in G-actin (Figure 5D). As with FH1FH2, the maximal extent of inhibition was ~50%. Because of the relatively low rate of nucleation by FH2, we could examine its effect on elongation as a function of G-actin concentration up to ~2 μM before nucleation affected the rates (Figure 5E). Within this range, the extent of inhibition was independent of G-actin concentration; the rate constant for elongation (the slope of this plot) always decreased by ~50% in the presence of 200 nM FH2. The extent of inhibition was similar with 15% or 75% of the actin labeled with pyrene (not shown). This confirmed that FH2 also partially capped the barbed end.

Capping factors can shift the critical concentration of actin by blocking the barbed end of the filament. Yet the critical concentration of the actin, indicated by the concentration giving no net elongation in Figure 5E or by the intercept of the fluorescence level achieved at steady state with the fluorescence at time 0, was not affected by FH2 (Figure 5F). Since the critical concentration was not raised, this confirms not only that the barbed end was only partially blocked by either construct, but also that the inhibition of elongation was not due to sequestration of G-actin or quenching of the pyrenylactin fluorescence.

FH1FH2 and FH2 Both Inhibit Depolymerization. Many but not all factors that inhibit elongation also inhibit depolymerization. To determine if FH1FH2 inhibited depolymerization, we examined the time course of depolymerization induced by addition of latrunculin A to sequester the free G-actin. Both FH1FH2 and FH2 (100 nM) decreased

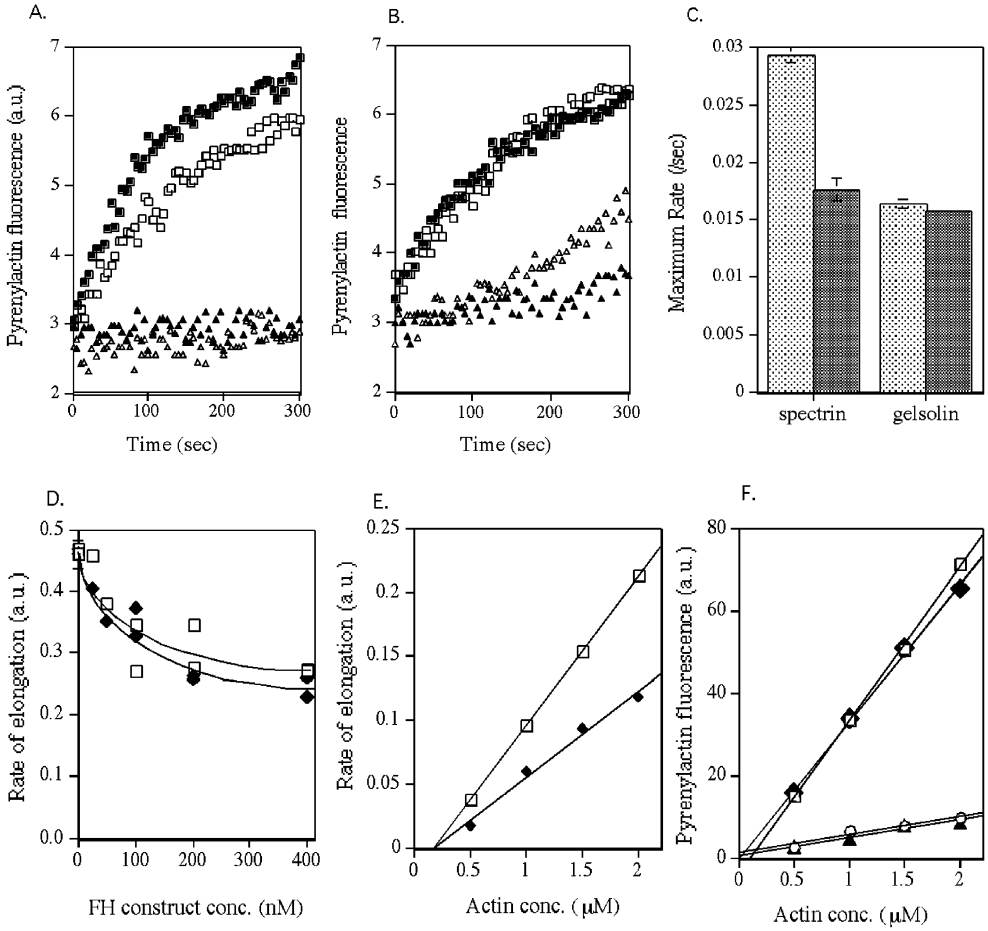

FIGURE 5: FH1FH2 and FH2 inhibit barbed-end elongation. (A) The time course of polymerization in the absence (triangles) or presence (squares) of spectrin actin seeds (~0.5 nM) in 1.2 μM actin (~1 μM above actin critical concentration; 50% pyrenylactin) was followed in the absence (filled symbols) or presence of 100 nM FH1FH2 (open symbols). Elongation was measured from the pyrenylactin fluorescence. Data are representative traces. (B) Time course of polymerization with (squares) or without (triangles) gelsolin−actin seeds (~5 nM) in 1.6 μM actin (~1 μM over gelsolin−actin critical concentration; 50% pyrenylactin) was followed in the absence (filled symbols) or presence of 100 nM FH1FH2 (open symbols). Polymerization was measured from the pyrenylactin fluorescence. Data are representative traces. (C) Initial rates of polymerization from spectrin seeds or gelsolin seeds (as in panels A and B) were measured without (light bars) or with FH1FH2 (dark bars). Data shown are the mean and range of duplicate samples. (D) Rate of polymerization from spectrin seeds as a function of FH1FH2 or FH2 concentration was determined from the initial rates of polymerization from spectrin actin seeds (~1 nM) in 0.5 μM G-actin (30% pyrenylactin) and different concentrations of FH1FH2 (open squares) or FH2 (closed diamonds). The data plotted are the initial rates as a function of the concentration of FH2 construct. (E) Rate of polymerization from spectrin seeds (0.5 nM) as a function of G-actin concentration (15% labeled) without (open squares) or with 200 nM FH2 (closed diamonds) was measured. The lines represent the best linear fits: for control, $y = 0.116x - 0.019$ ($r^2 = 1.000$); for FH2, $y = 0.067x - 0.011$ ($r^2 = 0.986$). (F) To determine the critical concentration of actin, the fluorescence of each sample in panel E was measured after 4 h. The line represents the best linear fit for samples without (open squares) or with 200 nM FH2 (closed diamonds). The critical concentrations ± FH2, are indicated by the intercepts of the lines for these end points of polymerization and the initial fluorescence for control (open circles) + FH2 (filled triangles). The data are from a representative experiment.

the rate of depolymerization by about 50% (Figure 6A). As with elongation, the effect appeared to saturate with partial inhibition (Figure 6C). Neither FH1FH2 nor FH2 inhibited pointed-end depolymerization from gelsolin-capped filaments (Figure 6B). The lack of effect on critical concentration, which reflects the net actin monomer off rate constant divided by the net on rate constant, is consistent with there being a partial inhibition of both the off and on rates.

DISCUSSION

FH1FH2-Induced Nucleation Occurs through Dimer Stabilization. Nucleation by FH1FH2 appears to occur by stabilization of an actin dimer. Dimer stabilization is also the likely mechanism of nucleation by capping protein (*10*) and cytochalasin (*9*). On the other hand, activated Arp2/3 complex nucleation appears to require only a single monomer (and a filament). Since the *n*-values are different, the relative activity of two nucleators will depend on the G-actin concentration, the one with the lower *n* (i.e., Arp2/3) working relatively better at low G-actin concentrations.

Dimer stabilization can occur either by capture of a spontaneously formed dimer or by sequential binding of two G-actin monomers. The former would be expected to be slow because of the very low concentration of dimers. Indeed, a conservatively high estimate of the maximal rate of filament production by this mechanism at 4 μM [G-actin] under the conditions of the experiment in Figure 1A falls short of that required to explain those data by a factor of nearly 3.[5] In view of the uncertainties of the

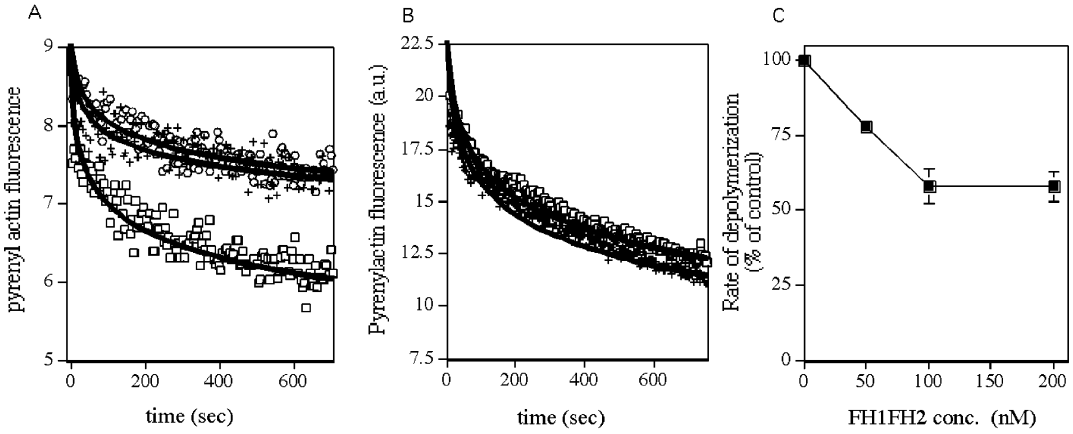

FIGURE 6: FH1FH2 and FH2 inhibit barbed-end depolymerization. (A) Actin filaments were polymerized overnight at 2.2 μM actin (15% pyrenylactin labeled). The filaments were sheared by passing through a 200 mL pipetman tip 10 min before the start of an assay when 100 nM FH1FH2 (plus symbols), 100 nM FH2 (open circles) or an equal volume of buffer (open squares) was added, and depolymerization was initiated by addition of 8 μM latrunculin A. The lines are the best fit for log plots and continued to fit a log plot up to 1200 s when the experiment was terminated. The presence of either FH1FH2 or FH2 decreased the rate by ~50%: control, $y = -1.15 \log(x) + 9.3$ ($r^2 = 0.86$); FH1FH2, $y = -0.68 \log(x) + 9.3$ ($r^2 = 0.64$); FH2, $y = -0.78 \log(x) + 9.6$ ($r^2 = 0.8$). (B) Gelsolin-capped filaments (0.2 μM gelsolin and 10 μM actin (30% pyrenylactin) incubated in polymerization buffer containing 0.1 mM $CaCl_2$). Depolymerization was induced by dilution to 2 μM actin into 8 μM latrunculin A in the absence (open squares) or presence of 100 nM FH1FH2 (plus symbols). The lines are the best fit log plot for control, $y = -5.087 \log(x) + 26$ ($r^2 = 0.95$); FH1FH2, $y = -5.091 \log(x) + 27$ ($r^2 = 0.95$). The difference between samples with and without FH1FH2 was less than the differences between duplicates (not shown). (C) Actin filaments were polymerized as in A and depolymerized by Lat A addition in the presence of different concentrations of FH1FH2. The curves were fit with Log plots as in A and data plotted are the ratio of rate constants in the presence of FH1FH2 relative to control. Error bars show the range of duplicates.

constants used this cannot be taken to rule out dimer capture as the mechanism, but it does make it appear unlikely. In contrast, similar calculations for sequential monomer addition lead to unidirectional fluxes 2 orders of magnitude greater and half-times of equilibration similarly shorter than needed to account for the observed rate of filament production with kinetics indistinguishable from the Tobacman/Korn model.[6]

FH1FH2-induced nucleation with pure actin is relatively inefficient. Under the conditions used, the number of filament ends produced was never more than 3% of the FH1FH2 molecules present. This contrasts with nucleation by low concentrations of activated Arp2/3 complex where the ratio of Arp2/3 to filaments can be 100% (*35*). The inefficiency of nucleation raises the question of how Bni1 functions in vivo in the presence of low G-actin concentrations (~0.5 μM). Bni1 does appear to nucleate in vivo (*16*, *20*), and FH1FH2 can nucleate filaments in yeast extracts without added actin. It is possible that additional factors in cytoplasm contribute to nucleation. This possibility is supported by the observation that cytochalasin, which also nucleates by dimer stabilization, is a more potent nucleator in cell supernatants than in pure actin (SHZ, unpublished observation). Alternatively, cofactors may activate formins to enhance nucleation just as activation of the Arp2/3 complex by WASP family members converts the mechanism of nucleation from dimer stabilization to one requiring only one G-actin (*1*, *11*). Finally, it is possible that a low efficiency of nucleation is sufficient for some cellular functions, especially since Bni1 is highly concentrated at the bud tip where actin cable nucleation occurs.

Enhanced Nucleation by Profilin−Actin. Profilin−actin contributed to FH1FH2-induced nucleation but less efficiently than free G-actin. Profilin interaction with the FH1 domain seemed essential, since H133S profilin−actin, which does not bind polyproline, did not enhance nucleation by FH1FH2 and wild-type profilin did not enhance nucleation by FH2. Nucleation induced by FH1FH2 was not affected by inclusion of 4 μM R74E profilin, which binds polyproline but not actin. This suggests that profilin−actin bound to the FH1 domain donates its actin to the nucleation site and does not merely produce a more active conformation of FH1FH2. Profilin decreases the lag time for nucleation slightly when Ca-actin is used (*3*); however, we observed little or no effect on the lag with Mg-actin (unpublished). Profilin could

[5] Any limitation of the ability of the rate of dimer capture (roportional to [G-actin]^2) to explain the rate of filament production (approximately proportional to [G-actin]^3) would be most apparent at higher [G-actin]. At 4 μM [G-actin], taking a low literature estimate of the dimer dissociation constant, 10^5 μM (*1*), the equilibrium dimer concentration would be 1.6×10^{-4} μM. Then using the maximal on-rate for FH1FH2 binding (diffusion-controlled rate constant 10/μM/s) and 75 nM FH1FH2 (as in Figure 1A) would lead to a maximum initial rate of filament production (ignoring any back reaction) of $10 \times 1.6 \times 10^{-4} \times 0.075 = 1.20 \times 10^{-4}$ μM/s. But the k_n obtained from the data (7.05×10^{-5} μM^3/s) predicts an initial rate of $7.05 \times 10^{-5} \times 0.075 \times 4^2 \times (4-0.1) = 3.30 \times 10^{-4}$ μM/s.

[6] Estimates of rates of filament production by sequential monomer addition are limitedby lack of information regarding the dissociation constant of the FH1FH2-monomer complex. Were the affinity as high as ~20 μM, we have the reaction

$$\text{FH1FH2} + \text{G-actin} \xleftrightarrow{20\,\mu\text{M}} \text{FH1FH2}-\text{G-actin} + \text{G-actin} \xleftrightarrow{3.55 \times 10^3\,\mu\text{M}} \text{FH1FH2}-(\text{G-actin})_2$$

with the second dissociation constant defined by k_n and the relationship given in Results. If we again assume diffusion-controlled on-rates, these reactions will have off-rate constants of 200 and 3.55×10^4/s respectively; thus, considered separately, half-times of equilibration of at most 3.47×10^{-3} and 1.95×10^{-5} s. At 4 μM [G-actin], their unidirectional fluxes at equilibrium will then be 2.5 and 0.5 μM/s, respectively. A difference between the forward and reverse fluxes of 3.30×10^{-4} μM/s (the rate of filament production predicted from the data of Figure 1A) would still leave the reactions essentially at equilibrium.

decrease the lag by enhancing the rate of cation exchange, however this would not account for the fact that profilin mutants unable to bind polyproline did not decrease the lag (*39*).

The contribution of profilin−actin to nucleation in vitro was small, raising the question why profilin is required in vivo for cable formation. Profilin−actin is presumably present in cells at a concentration considerably higher than free G-actin.[7] Thus, even if used less efficiently than free G-actin, in vivo profilin−actin may contribute significantly to nucleation. In addition, the profilin requirement for actin cable formation in vivo may result from the combination of an enhanced rate of nucleation and of filament elongation.

Comparison of FH1FH2 with FH2. In addition to allowing profilin−actin to contribute to nucleation, the FH1 domain also increased the efficiency of nucleation relative to FH2 alone. This effect was not due to the fact that the FH1FH2 was used as a GST fusion protein since removing the GST did not alter the activity of FH1FH2 (*2*). Furthermore, FH2 was equally effective at slowing kinetics of monomer addition or loss at the barbed end. Thus, the increased efficiency of nucleation by constructs containing the FH1 domain, with no difference in capping activity, suggests that the FH1 domain may contribute to the ability of FH2 to bind G-actin. FH1 does interact with actin via a yeast two-hybrid assay (*17*).

Barbed-End Capping by FH2. An interesting feature of the FH2 domain is that it maximally inhibits both barbed-end elongation and depolymerization by only 50%. This inhibition is limited to the barbed end. The inhibition could be due to slower rates of monomeric actin association and dissociation at the barbed end or to fewer available barbed ends. It is unlikely that this effect is due to incomplete saturation of the filament ends, since the rate of elongation remains 50% inhibited even when the concentration of FH2 is raised to several times its apparent K_d. While we have not ruled out the possibility that half of the filaments are totally capped and half uncapped and protected from capping, it is not easy to imagine how this would occur. An alternative possibility is that the filament ends are saturated with FH2 which functions as a "leaky" cap.

While the mechanism of leakiness is unclear, two possibilities can be pictured. (1) The binding of FH2 may occur at a site or sites such that it hinders but does not completely prevent both G-actin association and dissociation. (2) FH2 might bind with equal affinity in two different, mutually exclusive ways, one preventing elongation and depolymerization, the other having no effect on them. Under almost any model, FH2 must "walk" along a filament as it grows or shortens.

Why Does the Cell Use Arp2/3 for Nucleating Filaments under Some Conditions and Formins in Others? Actin filaments in nonmuscle cells serve both protrusive and contractile function. It is possible that the cell uses different mechanisms of nucleating actin, depending on whether the mechanical function of the new filament is to resist tension or compression. It has been argued that the dendritic branching pattern induced by the Arp2/3 complex is optimal for exerting protrusive force and resisting compressing (*1*). However, the structures dependent on formins; e.g., actin filaments in stress fibers, at attachment plaques and in the contractile ring, resist the tension of contraction. In yeast the actin cables must withstand the tension of myosin type V mediated vesicle transport. Perhaps the formin attachment to the barbed end is able to resist tension as it tethers the filament to a particular site.

[7] Since the K_d for profilin is ~0.1 μM, if the free [G-actin] is close to the pointed-end critical concentration ~0.5 μM, 80% of the profilin will be present as profilin−actin. While the profilin concentration in yeast is unknown, in mammalian cells it is in the micromolar range (~30 μM in neutrophils, Southwick and Young (1990) *J. Cell Biol. 110*, 1965−1973).

CONCLUSIONS

Actin nucleation by FH1FH2 appears to occur through actin dimer stabilization. While the FH2 domain is sufficient for this nucleation, addition of the FH1 domain increases the efficiency of nucleation and allows profilin−actin to contribute. The FH2 domain is sufficient on its own to mediate barbed-end capping. The capped barbed end shows a 50% decrease in both on rate and off rate with no net effect on the critical concentration. It is likely that the 50% inhibition of elongation and depolymerization are related to one another by some unknown mechanism.

ACKNOWLEDGMENT

We thank Rong Li for RLY574 and RLY1 yeast lines and E. Bi for YEF 473M; M. Joyce for excellent technical assistance and E. Bi, D. Pruyne, and A. Bretscher for helpful suggestions on the manuscript.

APPENDIX

Determination of Relationship between Maximal Rate of Polymerization and Nucleator Concentration. To derive equations that are soluble in closed form, we make the following assumptions:

1. the filament number concentration, [N], is always much smaller that the initial free G-actin concentration, $[G]_0$,
2. the free G-actin concentration, [G], is significantly greater than the critical G-actin concentration during the period of interest, and
3. FH1FH2 is not significantly consumed by the nucleation process, or by binding to the filaments formed.

Of these, the only one that does not obtain under some circumstances is the second. As a consequence, the equations derived below cannot reproduce a complete experimental time course to steady state. They do, however, describe the majority of the time course of experiments at the typical [G] values used to study nucleation.

Under these assumptions we can simplify the nucleation-elongation equations of Tobacman and Korn (1983), modified to include the role of FH1FH2 in stabilizing a nucleus of size $n - 1$, as

$$\frac{d[N]}{dt} = k_n[FH1FH2][G]^n$$

$$\frac{d[G]}{dt} = -k_+[N][G]$$

where k_+ is the elongation rate constant and k_n a composite nucleation-elongation constant. Adding these two equations appropriately weighted shows that

$$k_+[\mathrm{N}]\frac{\mathrm{d}[\mathrm{N}]}{\mathrm{d}t} + k_n[\mathrm{FH1FH2}][\mathrm{G}]^{n-1}\frac{\mathrm{d}[\mathrm{G}]}{\mathrm{d}t} = 0$$

and we obtain by integration

$$\frac{k_+}{2}[\mathrm{N}]^2 + \frac{k_n}{n}[\mathrm{FH1FH2}]([\mathrm{G}]^n - [\mathrm{G}]_0^n) = 0$$

Substituting this relationship into the differential equations, we obtain the solution

$$[\mathrm{N}] = \sqrt{\frac{2k_n[\mathrm{FH1FH2}][\mathrm{G}]_0^n}{nk_+}}\tanh\left(\sqrt{\frac{nk_nk_+[\mathrm{FH1FH2}][\mathrm{G}]_0^n}{2}}t\right)$$

$$[\mathrm{G}] = \frac{[\mathrm{G}]_0}{\cosh^{2/n}\left(\sqrt{\frac{nk_nk_+[\mathrm{FH1FH2}][\mathrm{G}]_0^n}{2}}t\right)}$$

From this it can be shown that the condition of maximal rate of conversion of G-actin to F-actin is

$$t = \frac{\sinh^{-1}(n/2)}{\sqrt{\frac{nk_nk_+[\mathrm{FH1FH2}][\mathrm{G}]_0^n}{2}}}$$

$$[\mathrm{G}] = \frac{[\mathrm{G}]_0}{\sqrt[n]{n/2+1}}$$

Thus, the maximal rate is given by

$$\left|\frac{\mathrm{d}[\mathrm{G}]}{\mathrm{d}t}\right|_{\max} = \left(\frac{[\mathrm{G}]_0}{\sqrt[n]{n/2+1}}\right)^{n/2+1}\sqrt{k_nk_+[\mathrm{FH1FH2}]}$$

Therefore we conclude that, under the nucleation-elongation model and the assumptions outlined above, the maximal rate is expected to occur at a constant value of [G] for any particular nucleus size and be proportional to the square root of the FH1FH2 concentration, whatever the nucleus size. A similar derivation leading to an equivalent, but less transparent, solution is given in Oosawa and Asakura (*34*).

REFERENCES

1. Pollard, T. D., Blanchoin, L., and Mullins, R. D. (2000) Molecular mechanisms controlling actin filament dynamics in nonmuscle cells, *Annu. Rev. Biol. Struct. 29*, 545−576.
2. Pruyne, D., Evangelista, M., Yang, C., Bi, E., Zigmond, S., Bretscher, A., and Boone, C. (2002) Role of formins in actin assembly: nucleation and barbed-end association, *Science 297*, 612−615.
3. Sagot, I., Rodal, A. A., Moseley, J., Goode, B. L., and Pellman, D. (2002) An actin nucleation mechanism mediated by Bni1 and profilin, *Nat. Cell Biol. 4*, 626−631.
4. Tobacman, L. S., and Korn, E. D. (1983) The kinetics of actin nucleation and polymerization, *J. Biol. Chem. 258*, 3207−3214.
5. Goode, B. L., Wong, J. J., Butty, A.-C., Peter, M., McCormack, A. L., Yates, J. R., Drubin, D. G., and Barnes, G. (1999) Coronin promotes the rapid assembly and cross-linking of actin filaments and may link the actin and microtubule cytoskeletons in yeast, *J. Cell Biol. 144*, 83−98.
6. Huttelmaier, S., Harbeck, B., Steffens, O., Messerschmidt, T., Illenberger, S., and Jockusch, B. M. (1999) Characterization of the actin binding properties of the vasodilator-stimulated phosphoprotein VASP, *FEBS Lett. 451*, 68−74.
7. Lambrechts, A., Kwiatkowski, A. V., Lanier, L. M., Bear, J. E., Vandekerckhove, J., Ampe, C., and Gertler, F. B. (2000) cAMP-dependent protein kinase phosphorylation of EVL, a Mena/VASP relative, regulates its interaction with actin and SH3 domains, *J. Biol. Chem. 46*, 36143−51.
8. Fievez, S., Carlier, M.-F., and Pantaloni, D. (1997) Mechanism of myosin subfragment-1-induced assembly of CaG-actin and MgG-actin into F-actin-S1-decorated filaments, *Biochemistry 36*, 11843−11850.
9. Tellam, R., and Frieden, C. (1982) Cytochalasin D and platelet gelsolin accelerate actin polymer formation. A model for regulation of the extent of actin polymer formation in vivo, *Biochemistry 21*, 3207−3214.
10. Caldwell, J. E., Heiss, S. G., Mermall, V., and Cooper, J. A. (1989) Effects of CapZ, an actin capping protein of muscle, on the polymerization of actin, *Biochemistry 28*, 8506−8514.
11. Mullins, R. D., Heuser, J. A., and Pollard, T. D. (1998) The interaction of Arp2/3 complex with actin: nucleation, high-affinity pointed end capping, and formation of branching networks of filaments, *Proc. Natl. Acad. Sci. U.S.A. 95*, 6181−6186.
12. Winter, D. C., Choe, E. Y., and Li, R. (1999) Genetic dissection of the budding yeast Arp2/3 complex: a comparison of the in vivo and structural roles of individual subunits, *Proc. Natl. Acad. Sci. U.S.A. 96*, 7288−7293.
13. Watanabe, N., et al. (1997) p140mDia, a mammalian homologue of Drosophila diaphanous, is a target protein for Rho small GTPase and is a ligand for profilin, *EMBO J. 16*, 3044−3056.
14. Tominaga, T., Sahai, E., Chardin, P., McCormick, F., Courtneidge, S. A., and Alberts, A. S. (2000) Diaphanous-related formins bridge rho GTPase and Src tyrosine kinase signaling, *Mol. Cell 5*, 13−25.
15. Riveline, D., Zamir, E., Balaban, N., Schwarz, U., Ishizaki, T., Narumiya, S., Kam, Z., Geiger, B., and Bershadsky, A. (2001) Focal contacts as mechanosensors: externally applied local mechanical force induces growth of focal contacts by an mDIA1-dependent and ROCK-independent mechanism, *J. Cell Biol. 153*, 1175−1186.
16. Evangelista, M., Pruyne, D., Amber, D. C., Boone, C., and Bretscher, A. (2002) Formins direct Arp2/3-independent actin filament assembly to polarize cell growth in yeast, *Nat. Cell Biol. 4*, 32−41.
17. Evangelista, M., Blundell, K., Lontine, M. S., Chow, C. J., Adames, N., Pringle, J. R., Peter, M., and Boone, C. (1997) Bni1p, a yeast formin linking Cdc42p and the actin cytoskeleton during polarized morphogenesis, *Science 276*, 118−122.
18. Kohno, H., et al. (1996) Bni1p implicated in cytoskeletal control is a putative target of Rho1p small GTP binding protein in *Saccharomyces cerevisiae*, *EMBO J. 15*, 6060−6068.
19. Imamura, H., Tanaka, K., Hihara, T., Umikawa, M., Kamei, T., Takahashi, K., Sasaki, T., and Takai, Y. (1997) Bni1p and Bnr1p: downstream targets of the Rho family small G-proteins which interact with profilin and regulate the actin cytoskeleton in *Saccharomyces cerevisiae*, *EMBO J. 16*, 2745−55.
20. Sagot, I., Klee, S., and Pellman, D. (2002) Yeast formins regulate cell polarity by controlling the assembly of actin cables, *Nat. Cell Biol. 4*, 42−50.
21. Frazier, J. A., and Field, C. M. (1997) Actin cytoskeleton: are FH proteins local organizers? *Curr. Biol. 7*, R414−417.
22. Wasserman, S. (1998) FH proteins as cytoskeletal organizers, *Trends Cell Biol. 8*, 111−115.
23. Pellam, R. J., and Chang, F. (2002) Actin dynamics in the contractile ring during cytokinesis in fission yeast, *Nature 419*, 82−86.
24. Schott, D. H., Collins, R. N., and Bretscher, A. (2002) Secretory vesicle transport velocity in living cells depends on the myosin-V lever arm length, *J. Cell Biol. 156*, 35−39.
25. Yang, H.-C., and Pon, L. A. (2002) Actin cable dynamics in budding yeast, *Proc. Natl. Acad. Sci. U.S.A. 99*, 751−756.
26. Young, C. L., Southwick, F. S., and Weber, A. (1990) Kinetics of the interaction of a 41-kilodalton macrophage capping protein with actin: promotion of nucleation during prolongation of the lag period, *Biochemistry 29*, 2232−2240.

27. Kouyama, T., and Mihashi, K. (1981) Fluorimetry study of N-(pyrenyl)iodoacetamide-labeled F-actin, *Eur. J. Biochem. 114*, 33−38.
28. Northrop, J., Weber, A., Mooseker, M. S., Franzini-Armstrong, C., Bishop, M. G., Dubyak, G. R., Tucker, M., and Walsh, T. P. (1986) Different calcium dependence of the capping and cutting activities of villin, *J. Biol. Chem. 261*, 9274−9281.
29. Cooper, J. A., Bryan, J., Schwab, B., Frieden, C., Loftus, D. J., and Elson, E. L. (1987) Microinjection of gelsolin into living cells, *J. Cell Biol. 104*, 491−501.
30. Casella, J. F., Maack, D. J., and Lin, S. (1986) Purification and initial characterization of a protein from skeletal muscle that caps the barbed ends of actin filaments, *J. Biol. Chem. 261*, 10915−10921.
31. Cano, M., Lauffenburger, D. A., and Zigmond, S. H. (1991) Kinetic analysis of F-actin depolymerization in polymorphonuclear leukocyte lysates indicates that chemoattractant stimulation increases actin filament number without altering the filament length distribution, *J. Cell Biol. 115*, 677−687.
32. Yang, C., Huang, M., DeBiasio, J., Pring, M., Joyce, M., Miki, H., Takenawa, T., and Zigmond, S. H. (2000) Profilin enhances Cdc42-induced nucleation of actin polymerization, *J. Cell Biol. 150*, 1001−1012.
33. Cooper, J. A., and Pollard, T. D. (1985) Effect of capping protein on the kinetics of actin polymerization, *Biochemistry 24*, 793−799.
34. Oosawa, F., and Asakura, S. (1975) *Thermodynamics of the Polymerization of Protein*, Academic Press, New York.
35. Higgs, H. N., Blanchoin, L., and Pollard, T. D. (1999) Influence of the C terminus of Wiskott-Aldrich syndrome protein (WASp) and the Arp2/3 complex on actin polymerization, *Biochemistry 38*, 15212−22.
36. Sept, D., Xu, J., Pollard, T. D., and McCammon, J. A. (1999) Annealing accounts for the length of actin filaments formed by spontaneous polymerization, *Biophys. J. 77*, 2911−2919.
37. Andrianantoandro, E., Blanchoin, L., Sept, D., McCammon, J. A., and Pollard, T. D. (2001) Kinetic mechanism of end-to-end annealing of actin filaments, *J. Mol. Biol. 312*, 721−30.
38. Bjorkegren-Sjogren, C., Korenbaum, E., Nordberg, P., Londberg, U., and Karlsson, R. (1997) Isolation and characterization of two mutants of human profilin I that do not bind poly(L-proline), *FEBS Lett. 418*, 258−264.
39. Goldschmidt-Clarmont, P. J., Machesky, L. M., Doberstein, S. K., and Pollard, T. D. (1991) Mechanism of the interaction of human platelet profilin with actin, *J. Cell Biol. 113*, 1081−1089.

BI026520J